

Mass Loss From Planetary Nebulae in Elliptical Galaxies

Joel N. Bregman and Joel R. Parriott

Department of Astronomy, University of Michigan, Ann Arbor, MI 48109

jrbregman@umich.edu

ABSTRACT

Early-type galaxies possess a dilute hot ($2 - 10 \times 10^6$ K) gas that is probably the thermalized ejecta of the mass loss from evolving stars. We investigate the processes by which the mass loss from orbiting stars interacts with the stationary hot gas for the case of the mass ejected in a planetary nebula event. Numerical hydrodynamic simulations show that at first, the ejecta expands nearly symmetrically, with an upstream bow shock in the hot ambient gas. At later times, the flow past the ejecta creates fluid instabilities that cause about half of the ejecta to separate and the other half to flow more slowly downstream in a narrow wake. When radiative cooling is included, most of the material in the wake ($> 80\%$) remains below 10^5 K while the separated ejecta is hotter ($10^5 - 10^6$ K). The separated ejecta is still less than one-quarter the temperature of the ambient medium and the only way it will reach the temperature of the ambient medium is through turbulent mixing (after the material has left the grid). These calculations suggest that a significant fraction of the planetary nebula ejecta may not become part of the hot ambient material. This is in contrast to our previous calculations for continuous mass loss from giant stars in which most of the mass loss became hot gas. We speculate that detectable OVI emission may be produced, but more sophisticated calculations will be required to determine the emission spectrum and to better define the fraction of cooled material.

Subject headings: galaxies: ISM — cooling flows — X-rays: galaxies — stars: mass loss

1. Introduction

Early-type galaxies can be luminous diffuse X-ray emitters where the emission is due to hot gas at $2 - 10 \times 10^6$ K (e.g., Athey 2003; Mathews & Brighenti 2003; Humphrey & Buote 2006; Diehl & Statler 2007). The origin of the hot gas is modeled as the normal mass loss

from an evolving old population, and possibly a smaller contribution due to infall of group or cluster gas. Stellar mass loss occurs during the evolutionary stages toward the top of the giant and asymptotic giant branches. This mass loss only partly defines the metallicity of the gas, as Type Ia supernovae will contribute at least as much mass in heavy elements (but an insignificant amount of hydrogen and helium). The stellar mass loss occurs at the velocities of the stars and once this gas is decelerated by its interaction with existing hot gas, it will have a temperature that is characteristic of the potential well of the galaxy. An additional source of heat is provided by supernovae, which may raise the gas temperature sufficiently so that some or all of the gas is gas flows out as a galactic wind. Galactic winds will dramatically lower the volume emission measure of the galactic gas, which is a leading explanation for galaxies with low luminosities of diffuse X-ray emission.

An important aspect of this model, the mass loss from stars into the galactic interstellar medium, needs to be understood as it affects the properties of the hot and cool gas in the galaxy. The metallicity of the hot medium is expected to result from the mass shed by stars plus SN Ia. The stellar metallicity of the bright ellipticals is about solar (Trager 2008), and if the relative abundance pattern is similar to the Galactic bulge stars (Zoccali et al. 2008), the lighter elements, such as oxygen or magnesium should be enhanced, relative to iron. However, the elemental abundance measurements in ellipticals, from XMM-Newton and Chandra X-ray data, show that oxygen is typically subsolar (Ji et al. 2009), less than anticipated by a factor of 2-4 (including the modest contribution of oxygen from SN Ia makes the discrepancy greater).

Stellar mass loss that does not become part of the hot ambient medium may simply remain neutral or warm ionized ($< 10^4$ K). Alternatively, it may become hotter (10^5 - 10^6 K), but cools radiatively, never becoming part of the ambient gas at 3 - 10×10^6 K (Fujita et al. 1996; Mathews 1990; Brighenti & Mathews 2005). This could occur because the mass loss from higher metallicity stars has a greater radiative loss rate, so higher metallicity gas cools radiatively and does not become part of the hot medium. In both cases, there may be observational consequences as such gas may produce detectable optical or ultraviolet emission lines.

To examine some of these issues, we began a series of numerical hydrodynamic calculations to study the fate of stellar mass in the hot gas environment of an early-type galaxy (Parriott 1998). In our first paper (Paper I, Parriott & Bregman 2008), we discussed the two-dimensional hydrodynamic code (a version of VH-1), the properties of the initial conditions, and a set of results for a mass-losing giant star. In particular, the mass loss rate was taken to be continuous in time at the rate $\dot{M}_{star} \approx 10^{-7} M_{\odot} yr^{-1}$, which is representative of stars along the giant and asymptotic giant branches. At this rate, the flow evolves to a

quasi-steady state on a timescale shorter than the mass-loss stage of these stars (the duration of our simulations is 3×10^6 yr).

When the stellar velocity is supersonic relative to the hot gas, a bow shock developed ahead of the star, imparting momentum to the stellar mass loss, producing a cool slowly-moving wake behind the star. There is a large velocity difference between the wake and the hot ambient gas, so Kelvin- Helmholtz instabilities develop, which leads to thermal mixing as well as shocks between these two components. In the absence of radiative cooling, the wake is heated to the ambient temperature of the hot medium within about 2 pc of the star. When radiative cooling is included, up to 25% of the wake remains cool by the time it exits the grid, 25 pc from the star. The fraction of cooled gas is lower for lower ambient pressures (densities) or higher stellar velocities, but the fraction of cooled gas was not tremendously sensitive to the metallicity of the stellar mass loss, at least for the parameters considered.

A second type of mass loss event occurs in stars, the planetary nebula (PN) stage, which is an impulsive mass loss event in the life of a star. The planetary nebula mass loss stage typically only lasts $\sim 10^3$ years, with mass loss rates near $\sim 10^{-4} M_{\odot} yr^{-1}$, and velocities ~ 10 km/s (Bedijn 1988; Frank, Balick, & Riley 1990). Although some details of the mass loss mechanism remain to be clarified, the timescale and the amount of mass loss are understood to the degree necessary for our purposes. Most studies agree that about $0.2 - 0.3 M_{\odot}$ is lost during the red giant and asymptotic giant stage, and another $0.1 - 0.2 M_{\odot}$ is lost in the planetary nebula shell (e.g., Boffi & Stanghellini 1994, Buckley & Schneider 1995). In this paper, we simulate the interaction between this planetary nebula shell and hot ambient medium through which it is moving.

2. Simulations

A detailed discussion of the hydrodynamic code is given in Paper I, so here we briefly summarize the nature of the calculation and the properties of the simulations considered.

2.1. Computational Method and Initial Conditions

Our two-dimensional hydrodynamic code, VH-1, was originally developed by the Virginia Institute of Theoretical Astrophysics (VITA) Numerical Astrophysics Group (Blondin & Lufkin 1993). It is based on a version of the Piecewise Parabolic Method Colella & Woodward (1984), but with changes to the geometry (spherical polar coordinates) and boundary conditions used here. Optically thin radiative losses are included through the time-independent

collisional ionization equilibrium cooling function, $\Lambda_N(T)$, of (Sutherland and Dopita 1993). This cooling function covers the temperature range $10^4 K - 10^{8.5} K$; for cooler gas, radiative losses are set to zero.

A non-uniform grid was utilized in order to have adequate resolution in the wake and at radii close to the planetary nebula. The outermost radius is 25 pc and at the innermost radius, 0.01 pc, where the ratio between the radius at $i+1$ and i is 1.01; there are 360 radial cells. The azimuthal cell spacing is chosen so that the wake, which develops along the polar axis, is described by about 100 cells, with the remainder of the azimuthal cells of nearly equal angular spacing. Fairly standard boundary conditions are employed and the code was converted to run in parallel mode, both topics being discussed in great depth in Paper I. A relevant detail is that there is outflow from the inner radial boundary, in order to permit mass loss.

There is a constant flow entering the grid from the left at a velocity of $v_{amb} = 350 \text{ km s}^{-1}$, which corresponds to a one-dimensional velocity dispersion $\sigma_* \approx 200 \text{ km s}^{-1}$. This velocity dispersion is representative of an intermediate luminosity galaxy. We set the temperature of the X-ray gas $T_{amb} = 3 \times 10^6 \text{ K} \approx 0.3 \text{ keV}$, also typical of a L_X galaxy. The density of the ambient gas is taken to be $n_{amb} = 10^{-3} \text{ cm}^{-3}$, which is a value found several kpc from the center of an X-ray luminous elliptical and within 1 kpc from the center of an X-ray poor galaxy.

We simulate the planetary nebula event by a step function increase in the mass loss rate at the inner radial boundary. This is accomplished by increasing the ejecta density by a factor of 10^3 for a duration of 5×10^3 years. The velocity and temperature input parameters for the ejecta remain at 35 km/s and 10^4 K , respectively. This results in an effective mass loss rate of $\sim 10^{-4} M_\odot \text{ yr}^{-1}$, for a total PN shell mass of $\sim 0.5 M_\odot$. We start this simulation using the results of our previous simulation in which the mass loss rate was constant at the pre-PN rate and run for 2×10^6 years (Paper I). This is an attempt to approximate a more realistic situation where the “superwind” is blown into a previously established wind. The post-PN mass loss rate (i.e. after 5×10^3 years) reverts back to $\sim 10^{-7} M_\odot \text{ yr}^{-1}$.

Since the mass of many PN shells are found to be near $0.1 M_\odot$, we will also carry out an additional set of simulations with a superwind phase that lasts only 10^3 years. The two choices of shell mass bracket the values observed for PNs.

2.2. Planetary Nebula Simulation Without Radiative Cooling

The evolution scenario for the gas from this simulated PN event begins with the initial mass loss stage as the thick shell slowly propagates outward. The mass loss becomes disrupted by the hot flow past the star and is advected downstream and off the grid. This entire process takes a physical simulation time of 6×10^5 years.

In order to accurately know how much of the cold PN gas is heated by the time it leaves the grid, we would need to mark the PN material and record the temperature of each parcel of gas as it exits the grid, but we did not implement this capability. Also, since this is a transient event we cannot use the time-averaged mass fluxes as we did for all of the previous quasi-steady state simulation analyses (Paper I). Rather, in addition to examining individual stages of the PN evolution, we will calculate an approximate heating efficiency by recording the total grid mass, and the mass flux through the outer grid boundary, as a function of time for both warm gas ($T_{amb}/4$) and cold ($T_{amb}/30$) gas temperature bins.

Beginning with the quasi-steady-state from the continuous mass loss solution (Figure 1), there is a well-established bow shock upstream of the star. Momentum transfer from the post-shock hot medium to the mass loss leads to the slow-moving wake. The high-velocity flow past the wake produces the cold extensions upward from the wake due to the excitation of Kelvin-Helmholtz instabilities. This leads to a combination of mixing and further shocks in the downstream region between the wake and the ambient flow, ultimately heating the wake and bringing it closer to the velocity of the hot ambient medium. Into this flow, the planetary nebula event occurs and is completed by 5×10^3 years (bottom panel of Figure 1, where it is a dense shell very close to the star).

This dense shell has enormous momentum compared to its surroundings, so it expands unimpeded for about 10^5 years. During this period, the location of the contact discontinuity moves upstream and the mass flux of shocked hot material increases (Figure 2). The interaction affects both the cool ejecta and the hot ambient medium. A reverse shock propagates into the planetary nebula ejecta, while the bow shock heats the dilute ambient material. These changes continue as the planetary ejecta expands, and by 5×10^4 years (bottom panel of Figure 2), the vertical extent of the ejecta has become larger than the original wake height. This modifies the downstream flow, changing the development of instabilities in the original wake, although those events are unimportant compared to the evolution of the much more massive PN ejecta.

At about 10^5 years, the shell reaches its maximum radius (about 2.5 pc in the upstream direction and 4 pc in the vertical direction) as the momentum density of the shell balances that of the post-shock ambient gas (top panel of Figure 3). A Rayleigh-Taylor instability

has begun to grow along the leading edge. The low density post-PN wind behind the dense PN shell has a low temperature of order $\sim 10^2$ K, and a pressure several orders of magnitude below that of the post-shock ambient gas. A circular back-flow develops in the dilute ambient gas downstream of the PN ejecta, which will have a disruptive effect as the ejecta further expands. By 2×10^5 years (bottom panel of Figure 3), the leading edge instabilities have completely broken through the PN shell, allowing the ambient gas to enter the bubble and to disrupt the nebula. The ambient wind has imparted considerable momentum to the nebula and accelerated its velocity to about half the ambient value, so the disruption of the PN continues as the entire structure moves downstream at ~ 150 km/s, although the base remains loosely attached to the main downstream wake.

By 3×10^5 years (Figure 4), the base of the nebula is roughly half way downstream to the numerical boundary. The head of the nebula is still attached to this base, but ambient gas continues to shock and penetrate the cloud on the leading edge. A large vortex has been established on the back side of the nebula. This is the last output time where almost all of the PN gas is still entirely on the grid. At 4×10^5 years (bottom panel in Figure 4), the slower moving left-side structure from the previous figure has been completely separated from the rest of the nebula. This blob has risen more than 10 pc above the symmetry axis, and is about to exit the grid. There has been significant thermal heating through shocks between the blob and the more rapidly flowing ambient medium as well as through the mixing of the ejecta with the hot ambient gas. In this detached cloud, there is no gas cooler than 10^5 K. Although some of the original PN material still resides in the slower moving wake, well over half of the nebula has left the grid by the next figure at 5×10^5 years (top panel in Figure 5). The PN ejecta has nearly all left the grid by 5×10^5 (bottom panel in Figure 5) and the flow is returning to the quasi-steady properties of the pre-ejecta situation.

In trying to quantify the heating of the PN ejecta, we examined the following quantities, taken every 10^4 years, and for the gas at or below the temperature cutoffs of $T_{amb}/4 = 7.5 \times 10^5$ K, and $T_{amb}/30 = 10^5$ K: the stellar wind mass loss rate; the total grid mass; and the mass flux through the outer grid boundary. The methods of computing the mass fluxes were described in Paper I. The total grid mass was computed by summing the product of the mass density and the cell volume for each cell with a temperature below the given temperature cutoff. The background level of wake material present from times before and after the PN superwind phase cannot be distinguished from the nebula material, but this is only a $\sim 4 - 10\%$ effect since the wake mass is so small compared to the PN shell mass.

The mass flux and total gas mass below a temperature of $T_{amb}/4 = 7.5 \times 10^5$ K is shown in Figure 6 (we will refer to this as warm gas, and as we show, it is dominated by gas in the range $1 - 7.5 \times 10^5$ K). Due to the temperature threshold, these quantities exclude the

ambient gas that was heated by the bow shock. We have also included some simulation data from 10^5 years before the PN superwind phase in order to establish the background level of wake material. This figure quantifies the major features of the simulations: there is a time lag of 3×10^5 years between the PN superwind phase and the increase of the exiting mass flux above the background level (indicating the bulk departure of the PN material). The total grid mass data also confirms a background warm gas grid mass level of $\sim 0.02M_\odot$, prior to the PN event that releases $0.5M_\odot$. At least half of the PN ejecta still lies below 7.5×10^5 K, four times cooler than the ambient material. The large piece of the nebula that leaves the grid at 4×10^5 years has a mass of $\approx 0.25M_\odot$, and additional warm material leaves the grid near the center of the wake.

We also consider the mass of material that is closer to the temperature of the ejecta (10^4 K) by calculating the same quantities for gas at a temperature below $T_{amb}/30 = 10^5$ K gas (Figure 7; referred to as cold gas). The initial shock that is propagated into the PN ejecta heated about three-quarters of the gas above 10^5 K. Once instabilities became well-developed, at about 10^5 years, the remaining cold gas was quickly heated so that by 2.3×10^5 years, there is no significant amount of cold gas beyond the amount present prior to the PN event. To summarize, in the interaction between the PN ejecta and the rapidly-moving hot ambient material, the temperature of the ejecta has been raised by a factor of 50-100 by the time it exits the grid. It still is a factor of several below the hot ambient medium, where the temperature rose due to the bow shock interaction. Below, we comment on the likely fate of the warm gas once it leaves the grid.

2.3. Planetary Nebula Simulation with Cooling

In the continuous mass loss case (Paper I), the addition of radiative cooling changed the structure, as well as the temperature distribution of the mass shed by the star. One change was that the Kelvin-Helmholtz and Rayleigh-Taylor instabilities develop more rapidly and closer to the star, as is seen in Figure 8, which forms the initial conditions for this run. A second change was that the wake became thinner and cooler, with 15% of stellar ejecta exiting the grid as cool material ($T < 10^5$ K).

Despite the difference in the initial conditions, the dominant feature for the first 5×10^5 years is the expansion of the PN ejecta, although the timescales (or sizescales) are a bit accelerated for the case with radiative cooling. For the radiative cooling case, instabilities develop that cause the ejecta event to extend to larger vertical heights and this provides a larger cross section to the incoming shocked hot flow (Figure 9). In turn, the larger cross section leads to a larger amount of momentum transfer, as well as a greater mass of shocked

ambient material.

By 10^5 years, the momentum transfer has pushed the ejecta upward (to about 6 pc) and downstream, with a number of instabilities developing in the leading surface of the PN ejecta. In the subsequent 10^5 years, the development of fluid instabilities and momentum transfer have accelerated (bottom panel of Figure 10). The most striking structures are those that have nearly entirely broken away from the flow closer to the wake. These extended structures lie about 17 pc above the wake as they approach the downstream boundary, 25 pc from the star. The pieces of PN ejecta that are furthest from the star have received the most momentum and energy transfer, so one expects them to have a higher mean temperature than the material in the wake and closer to the star. This expectation is realized and when we calculate the mass of the of this nebula material that is moving off the grid at about 2×10^5 years, we find a mass of $\approx 0.2M_\odot$ below 7.5×10^5 K, and $\approx 0.02M_\odot$ of that amount is below 10^5 K. The last of the larger warm/cool structures is about to exit the grid at 3×10^5 years (Figure 11), and the bulk of the PN material appears to be gone by 4×10^5 years. While this amount of cool gas may seem rather small, it is significant in comparison to the simulation without radiative cooling, where there was no cool gas in the exiting ejecta fragments. Also, it is possible that radiative cooling will become more important in this cool gas as it flows further downstream.

In addition to the highly extended and detached structures, a significant amount of cool gas remains in the wake region directly behind the star. Momentum transfer and mixing in this region is slower, so radiative losses more easily balance the energy input, leading to a larger fraction of cool gas (and a longer time to flow off the grid). The warm and cold gas mass flux data are shown in Figures 13 and 14, respectively. The time-lag between the PN event and the increase in exiting mass flux is 1×10^5 years shorter than in the adiabatic case due to the increased rate of momentum transfer. The two large spikes in the exit flux curve at 2.1×10^5 years and 2.5×10^5 years are the two large warm/cool features close to the edge of the grid in the 2×10^5 year contour map (Figure 10). The total mass and exit flux curves suggest that all of the warm gas ($< 7.5 \times 10^5$ K and $> 10^5$ K) has left the grid by 3.5×10^5 years.

The amount of cool material is changing with time, so we estimate of the relative cooled mass by integrating under the warm and cold exiting mass flux curves in two intervals from 2×10^5 years to 3.5×10^5 years, and from 3.5×10^5 years to 6×10^5 years. Since the first interval contains the exiting large structures, the bulk of the gas in this interval is warm. The second interval shows a growing cold wake, with the majority of the gas exiting in this interval being cold ($< 10^5$ K). The values that we obtain confirm this: the percentage of cold gas leaving the grid in the first interval is $\approx 3\%$; the percentage for the second interval

is $\approx 80\%$. The cold fraction for the full 2×10^5 to 6×10^5 year interval, which covers the bulk of the time when PN material is leaving the grid, is $\approx 30\%$. These values as well as the total grid mass data suggest that although the warmer PN material quickly exits the grid, radiative cooling is able to keep a significant fraction of the PN material in the slower wake region and cold. This is twice the amount of cool gas that exits the grid in the continuous mass loss case (Paper I).

2.4. Reduced Planetary Nebula Masses

Our $0.5M_\odot$ planetary nebula simulation has roughly twice the mass that is often found in a PN shell. Although we do not expect this difference in shell mass to effect the general nature of the PN evolution, we have run another set of simulations where the superwind phase lasts only 10^3 years, resulting in a $0.1M_\odot$ shell. These two mass loss events bracket the typical PN shell masses observed.

2.4.1. Simulation Without Radiative Losses

The evolution of this simulation is very similar to that where the PN ejecta is $0.5M_\odot$, with just a few differences. The rate of momentum transfer from the ambient flow to the PN ejecta is greater than in the $0.5M_\odot$ case. This is because the mass of the ejecta increases as r^3 while the area with which it interacts with the ambient flow increases as r^2 , so the velocity of the ejecta increases as $M_{ejecta}^{-1/3}$. Due to the increased momentum transfer, most of the gas exits the grid by 3×10^5 years. Because the evolution is so similar to the $0.5M_\odot$ case, we will only include the grid state at 2.5×10^5 years which shows the main part of nebula almost about to leave the grid (Figure 15). Upon exiting the grid, the main nebula structures are accelerated up to ≈ 300 km/s, close to the speed of the ambient material. The velocity difference between these nebular features and the hot ambient medium is less than the sound speed in either medium, so subsequent heating of that gas will occur primarily through turbulent mixing.

An examination of the mass flux curves (Figures 16 and 17) show that the detached PN ejecta feature exits the grid at $2 - 3 \times 10^5$ years while the component in the narrower wake exits at $3.5 - 5.5 \times 10^5$ years. Both components contain warm gas but neither contain cool gas, which is similar to the higher mass ejecta case.

2.4.2. *Simulation With Radiative Losses*

As with the $0.5M_{\odot}$ case, the instabilities are much stronger and more numerous than in the simulation without radiative losses, but the cooling compresses many of these fingers and the wake so that they do not heat up to the ambient temperature. Figure 18 shows maps of the cooling run at 1×10^5 years and 1.5×10^5 years. The top panel shows the typical unstable nature of the ejecta with cooling included, and just 0.5×10^5 years later the bulk of the PN has broken off completely. It exits the grid at ≈ 250 km/s, less than in the case without radiative losses and this is probably due to the smaller cross section that results from the additional compression of the cooler gas. A large component of the nebula ejecta remains in the wake, remaining cooler and moving more slowly at the same timestep.

The warm and cold mass flux curves (Figures 19 and 20) confirm that the cooled gas moved off the grid more quickly than in the non-cooling case and the ejecta is broken up into smaller parcels. The sharp peak around 2×10^5 years in the exiting mass flux curve shows the exit of the large component that had broken off (Figure 18). A comparison of the cold and warm exit mass flux curves shows that this piece contains only warmer gas as it exits this simulation. However, the velocity difference between this gas parcel and the ambient medium is about 100 km/s, so most of the energy and momentum has been transferred to this gas. If further momentum transfer were to erase the velocity difference with the ambient medium, the additional thermal heating of the cloud would only raise the temperature modestly. This would still be at least a factor of three cooler than its surroundings and radiative cooling would reduce the temperature, making this a cold cloud. The remainder of the PN material lies in the less rapidly moving wake, which continues to cool radiatively as it moves downstream. The fraction of cold gas leaving the grid between 2×10^5 and 6×10^5 years is about $\approx 40\%$. However, excluding the departure event at 2×10^5 years, $\approx 75\%$ of all the gas that leaves the grid has a temperature below 10^5 K.

3. Discussion and Conclusions

We simulated the interaction between the mass loss from stars during their planetary nebula stage and the hot medium of an early-type galaxy. It is necessary to model this common interaction if one is to understand the evolution of hot and cold gas in these galaxies. About half the mass shed by old stars occurs continuously, although at varying mass loss rates, during the ascent up the giant and asymptotic giant branch, which we modeled in Paper I. The other half of the mass loss occurs as a relatively rapid event, the birth of a planetary nebula, and that stage is modeled here. We simulated the ejection of the planetary nebula shell with and without radiative losses in order to separate the physical events related

to each. For a summary, we will focus on the simulations with radiative losses.

For most previous and the current simulations, the flow past the star is supersonic, so a bow shock develops, which shocks both the fast ambient flow and the stellar mass loss. For the previous continuous mass-loss simulations, the mass loss expanded until the momentum of the ejecta approached that of the fast but dilute ambient medium. The momentum transfer of the shock caused stellar mass loss to flow downstream, creating a wake, which is subject to Kelvin-Helmholtz and Rayleigh-Taylor instabilities. Shocks propagate into the dense extensions created by these instabilities, producing significant heating.

In the planetary nebula simulations, the ejecta expands to about 3 pc before reaching a comparable value to the momentum density of the fast flow. Moving around this expanded ejecta is the flow of the post-shock hot gas, which excites instabilities of several wavelengths, but the dominant mode is one that is similar to the size of the expanded ejecta. About half of the ejecta becomes extended vertically relative to the initial direction of the fast flow. This increases the cross section for momentum transfer and that cooler material is accelerated downstream and heated through shocks into the originally cool ejecta. By the time the detached ejecta flows through the boundary of the computational grid (25 pc from the star), it is moving between 50-70% of the velocity of the background flow. However, the temperature of the gas is less than 25% that of the pre-shock ambient gas. The additional heating that would occur by having the cloud reach the ambient hot gas velocity is insufficient to bring it to the temperature of the ambient dilute medium. This component of the ejecta will radiatively cool, provided that the hotter ambient medium does not mix in at a rate that exceeds the radiative cooling rate. Our simulation cannot address this issue.

Approximately half of the planetary nebula ejecta flows back behind the star as a cool wake that moves at about half the speed of the detached ejecta. The fast flow past the wake excites fluid instabilities that lead to shocks being driven into the gas as well as thermal mixing between the wake and the surrounding ambient medium. The rate of heating associated with these processes is less than the radiative cooling rate, so the most of the wake material (> 80%) remains cool (< 10^5 K). At the exit boundary, 30-40% of the total mass of the ejecta is still cool, which is at least double the amount from the comparable continuous mass loss case of Paper I (15%). If there is additional radiative cooling of this ejecta beyond the computational boundary, as argued above, most of the mass of the ejecta from a planetary nebula may remain cool. These results suggest that continuous stellar mass loss, during the giant stages, is more likely to become the hot ambient interstellar medium than the ejecta from planetary nebula, which is more likely to remain cool.

The amount of remaining cool ejecta results from a balance between radiative losses and fluid heating processes. The radiative loss rate depends upon the metallicity, so higher

metallicity gas is likely to remain cool. This code does not have the ability to give one component of the fluid a different metallicity (the ejecta), while keeping the hot ambient flow unchanged. Therefore, we could not carry out a simulation to investigate this point. From our previous simulations (Paper I), we found that the results did not always change as anticipated or by the magnitude that one might infer from simple estimations. From these experiences, a careful simulation will be needed to address the metallicity issue.

One of the suggestions presented in Paper I is that at least some of the optical emission line gas (at $\sim 10^4$ K) that is seen in early-type galaxies is the cool mass loss from evolving stars. Gas emitting at higher temperatures, such as OVI, is seen in observations obtained by the FUSE satellite (Bregman et al. 2005). The ion OVI exists primarily in the $2 - 5 \times 10^5$ K temperature range, and this is similar to the temperatures found in the wake and the detached ejecta (or the gas has passed through this range in cooling). The observed OVI line fluxes has been interpreted as indicative of gas cooling from the ambient temperature though the OVI temperature range (and eventually to 10^4 K or lower (Edgar & Chevalier 1986); this is a cooling flow model). Our calculations suggest that an alternative explanation is possible: the collective transient heating of stellar ejecta to the OVI temperature range. Unfortunately, non-equilibrium ionization effects are important in this temperature range, so to calculate the OVI line fluxes accurately, one will need to follow the ionization properties of every fluid element, which is well-beyond the capabilities of our calculations.

While our calculations indicate certain types of behavior for the mass loss from stars, it will require a more ambitious set of calculations to properly determine the fractional mass of cool gas and the emission line strengths. Of central importance has been the strength and evolution of fluid instabilities, but in our calculation, the fluid is treated in two spatial dimension, with symmetry in the third (angular) coordinate. This may change the growth rate of instabilities, and consequently, the evolution of the stellar ejecta. Another improvement would be simulations that could follow the late time evolution of the stellar ejecta (beyond our grid boundaries), and even the evolution of the material as it begins to fall inward in the galaxy. An important addition would be the ability to identify the stellar mass loss (as opposed to the ambient material) and for the ejecta to have a different metallicity than the ambient gas. Lastly, a larger grid of simulations is warranted, such as simulations in which the ambient pressure is significantly larger, such as in the central few hundred pc of a galaxy.

JRP would like to give special thanks to Philip Hughes and Hal Marshall for their valuable advice and comments during code development, simulations, and on the content of my PhD Thesis. Also, thanks are due to Gus Evrard and Douglas Richstone for serving on JRP's thesis committee and for providing timely support and advice. Financial support is

gratefully acknowledged and was provided to JRP through a Department of Energy Computational Science Graduate Fellowship and to JNB through a Long Term Space Astrophysics Grant from NASA.

REFERENCES

- Athey, A.E. 2003, Ph.D. Thesis, University of Michigan.
- Bedijn, P. J. 1988, *A&A*, 205, 105
- Blondin, J. M., & Lufkin, E. A. 1993, *ApJS*, 88, 589
- Boffi, F. R., & Stanghellini, L. 1994, *A&A*, 284, 248
- Bregman, J. N., Miller, E. D., Athey, A. E., & Irwin, J. A. 2005, *ApJ*, 635, 1031
- Brighenti, F., & Mathews, W. G. 2005, *ApJ*, 630, 864
- Buckley, D., & Schneider, S. E. 1995, *ApJ*, 446, 279
- Colella, P., & Woodward, P. R. 1984, *Journal of Computational Physics*, 54, 174
- David, L. P., Jones, C., Forman, W., Vargas, I. M., & Nulsen, P. 2006, *ApJ*, 653, 207
- Diehl, S., & Statler, T. S. 2007, *ApJ*, 668, 150
- Edgar, R. J., & Chevalier, R. A. 1986, *ApJ*, 310, L27
- Frank, A., Balick, B., & Riley, J. 1990, *AJ*, 100, 1903
- Fujita, Y., Fukumoto, J., & Okoshi, K. 1996, *ApJ*, 470, 762
- Hardee, P. E., & Stone, J. M. 1997, *ApJ*, 483, 121
- Humphrey, P. J., & Buote, D. A. 2006, *ApJ*, 639, 136
- Irwin, J., Sivakoff, G. R., Sarazin, C. L., Ji, J., Bregman, J. N., & Mathews, W. G. 2006, *American Astronomical Society Meeting Abstracts*, 209, #04.14
- Ji, J., Irwin, J. A., Athey, A., Bregman, J. N., & Lloyd-Davies, E. J. 2009, *ApJ*, 696, 2252
- Mathews, W. G. 1990, *ApJ*, 354, 468
- Mathews, W. G., & Brighenti, F. 2003, *ARA&A*, 41, 191

- Parriott, J.R. 1998, Ph.D. Thesis, University of Michigan.
- Parriott, J. R., & Bregman, J. N. 2008, ApJ, 681, 1215
- Sutherland, R. S., & Dopita, M. A. 1993, ApJS, 88, 253
- Trager, S. C. 2008, The Metal-Rich Universe, 141
- Xu, J., Hardee, P. E., & Stone, J. M. 2000, ApJ, 543, 161
- Zoccali, M., Lecqueur, A., Hill, V., Barbuy, B., Renzini, A., Minniti, D., Gómez, A., & Ortolani, S. 2008, Memorie della Societa Astronomica Italiana, 79, 503

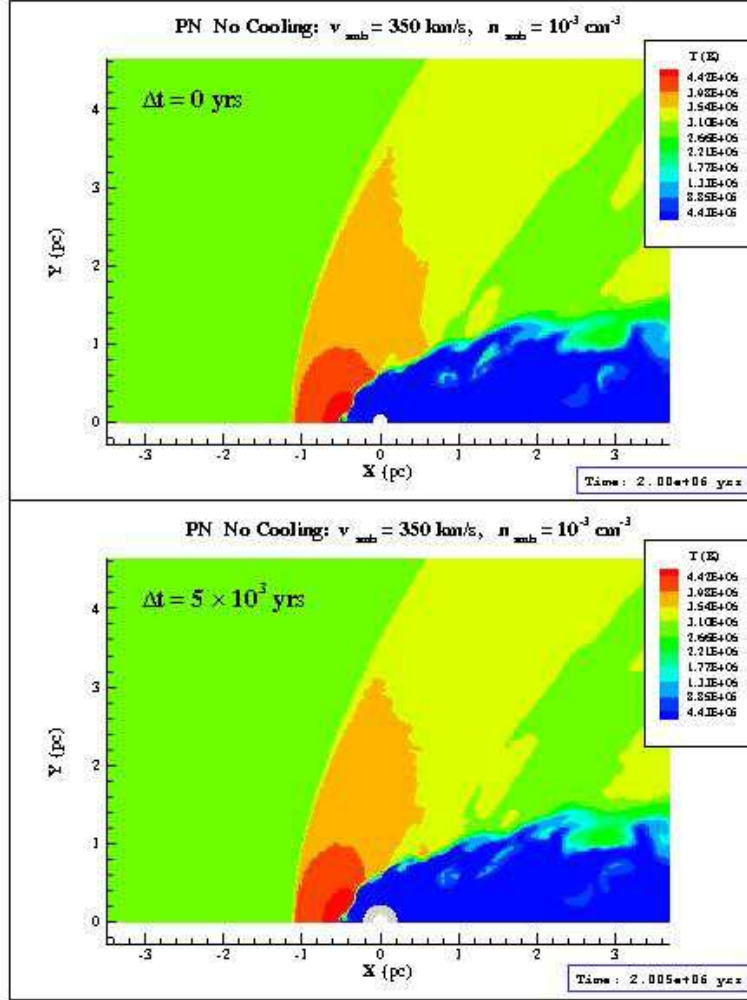


Fig. 1.— The beginning of the PN evolution just before (top) and just after (bottom) the impulsive superwind phase. Prior to the PN ejection event, the star was losing mass at a rate of $\sim 10^{-7} M_{\odot} \text{ yr}^{-1}$, typical of a AGB star. At this point, the cool wake material is from this AGB stage. The velocity difference between ambient hot material and the star is 350 km s^{-1} , which leads to the bow shock on the upstream side of the flow.

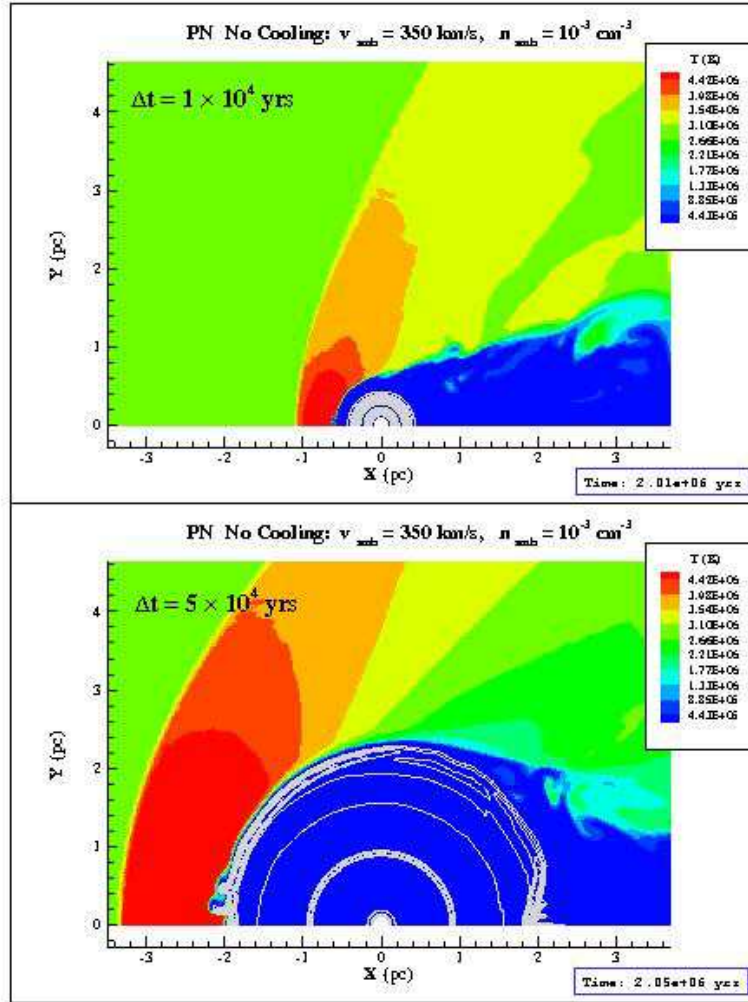


Fig. 2.— Continuing outward flow of the dense PN shell before coming into ram pressure equilibrium with the ambient flow. The times are at 10^4 and 5×10^4 years after the start of the superwind.

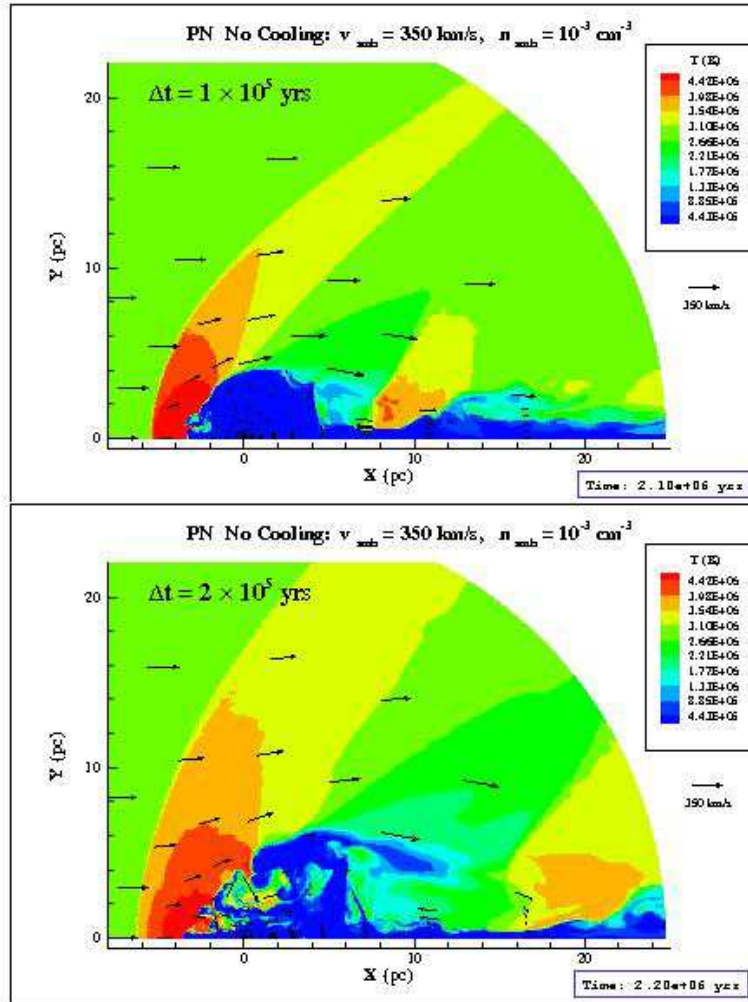


Fig. 3.— Shell expansion ceases and instabilities begin to grow by 10^5 years (top). The ambient flow has produced instabilities in the leading edge of the PN shell. Disruption of the ejecta is well underway by 2×10^5 years (bottom).

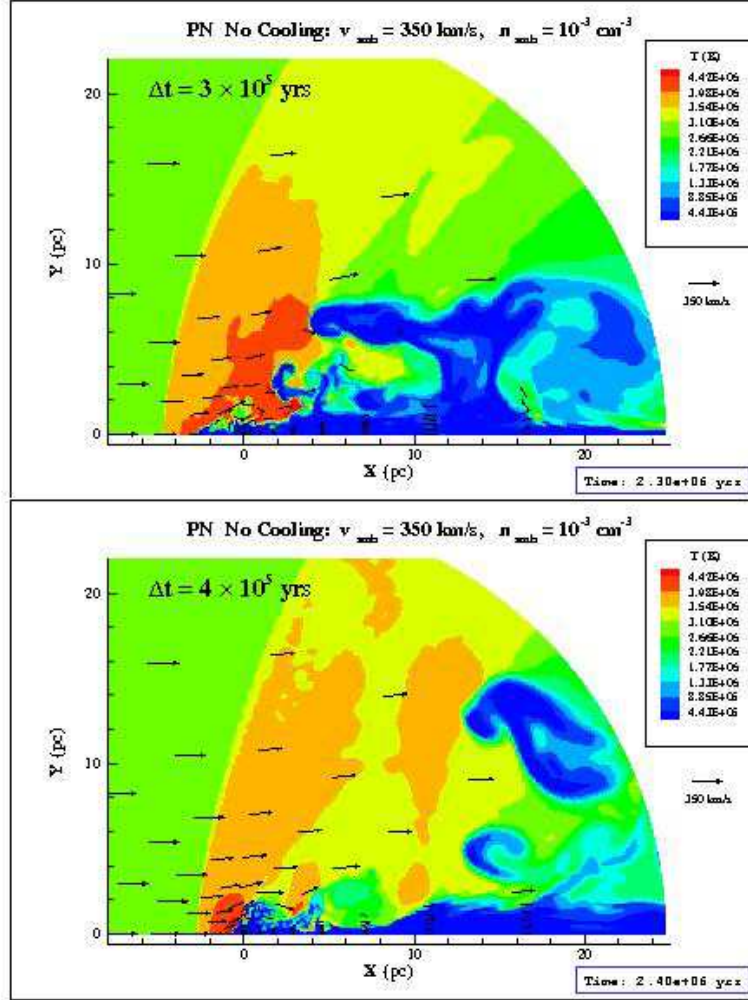


Fig. 4.— The disrupted PN is accelerated downstream and off the grid by momentum transfer from the ambient gas. Although there is still a tenuous connection to the wake, the bulk of the nebula is moving off the grid with a velocity of half the ambient value. The output at 3×10^5 years (top) is the last one with the full nebula still on the grid. By 4×10^5 years (bottom) one large warm piece of nebula material, with mass $\approx 0.25M_{\odot}$ or half the original PN mass, has separated and the rest of the PN has been advected off the grid. There is PN material still in the slower-moving wake.

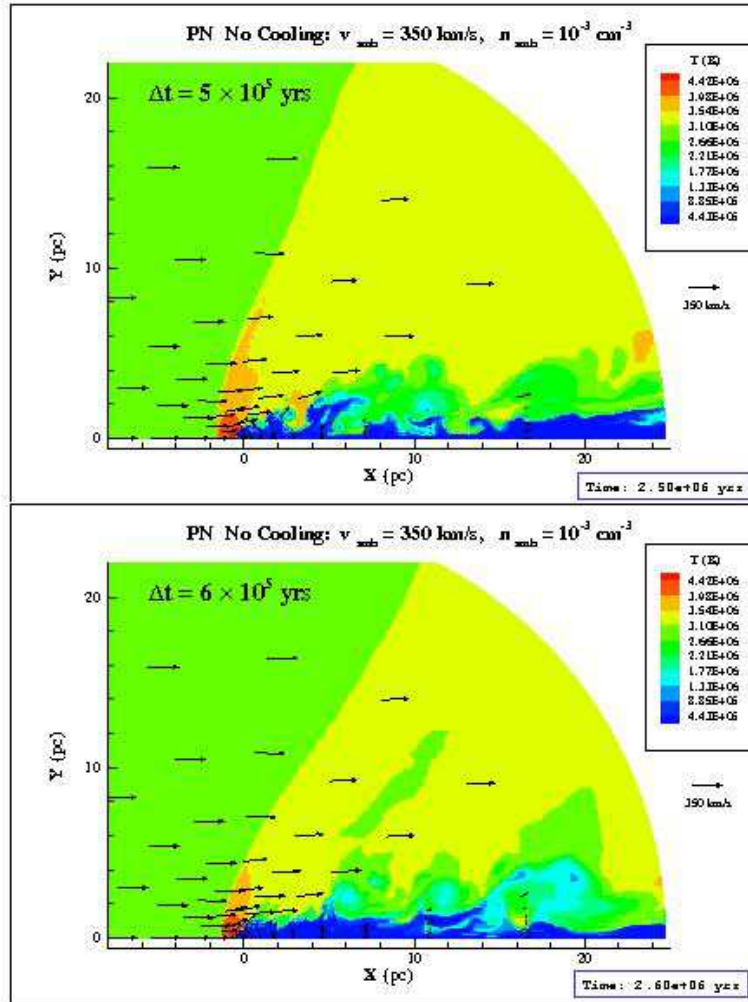


Fig. 5.— The majority of the PN has exited the grid, although some material may remain in the slow wake. By 6×10^5 years (bottom), the flow has nearly returned to its pre-PN state.

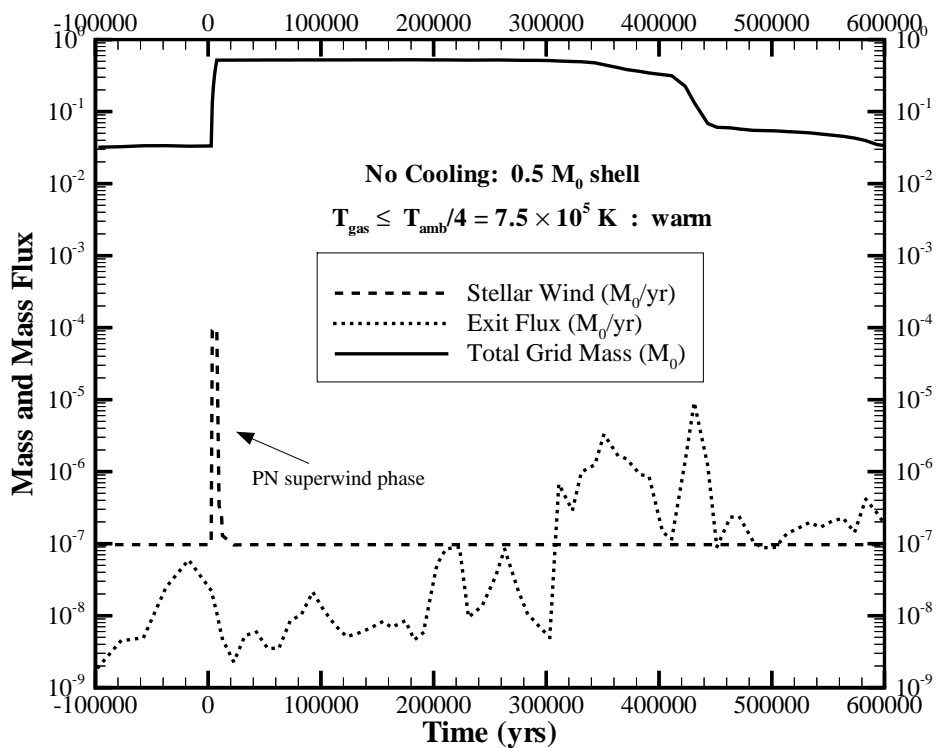


Fig. 6.— Mass fluxes for warm $< T_{\text{amb}}/4$ K gas. The total mass and exiting mass flux data suggest that a large fraction of this warm PN-material is not heated to ambient temperatures by the time it leaves the grid. The bulk of the nebula begins to exit the grid 3×10^5 years after the superwind.

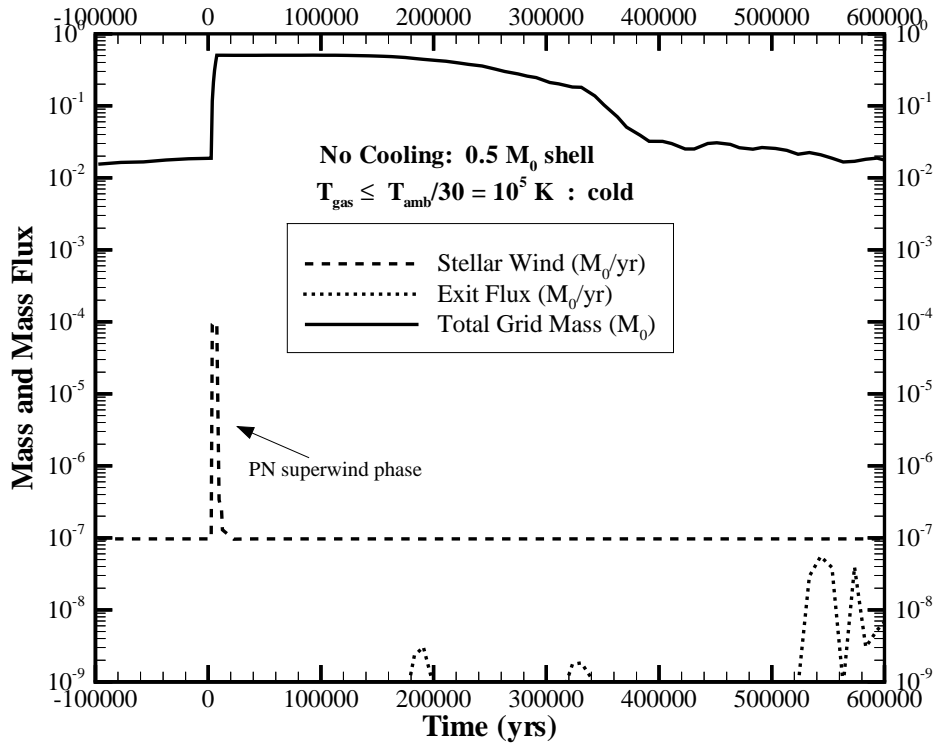


Fig. 7.— Mass fluxes for colder $< T_{\text{amb}}/30$ K gas. These curves suggest that this cooler gas is heated by the time it leaves the grid, as we would expect for an adiabatic flow.

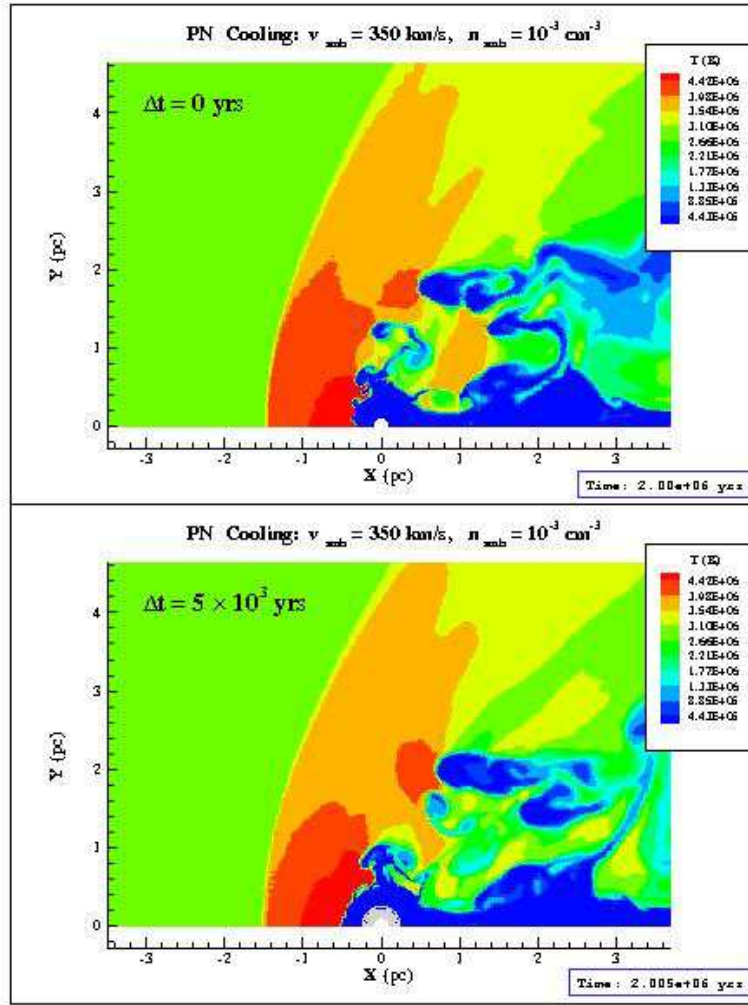


Fig. 8.— The beginning of the PN evolution just before (top) and just after (bottom) the impulsive superwind phase. The cooled flow is more complex, as discussed with previous simulations.

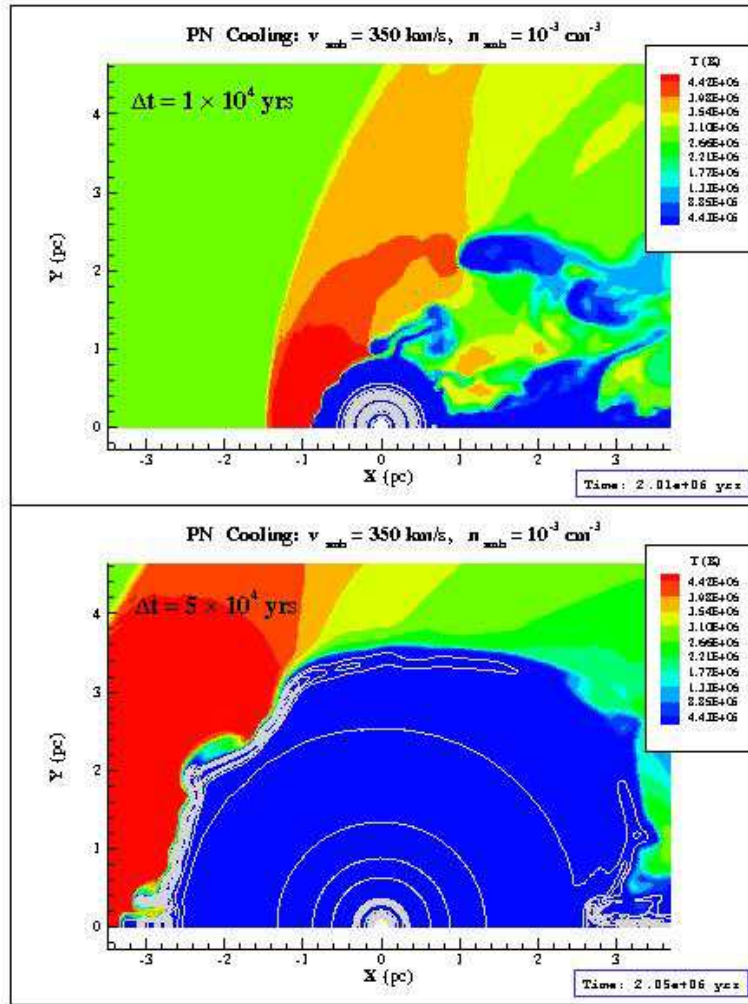


Fig. 9.— The outward flow of the dense PN shell continues before coming into ram pressure equilibrium with the ambient flow. The times are at 10^4 and 5×10^4 years after the start of the superwind. There are more growing leading-edge instabilities in this cooled case.

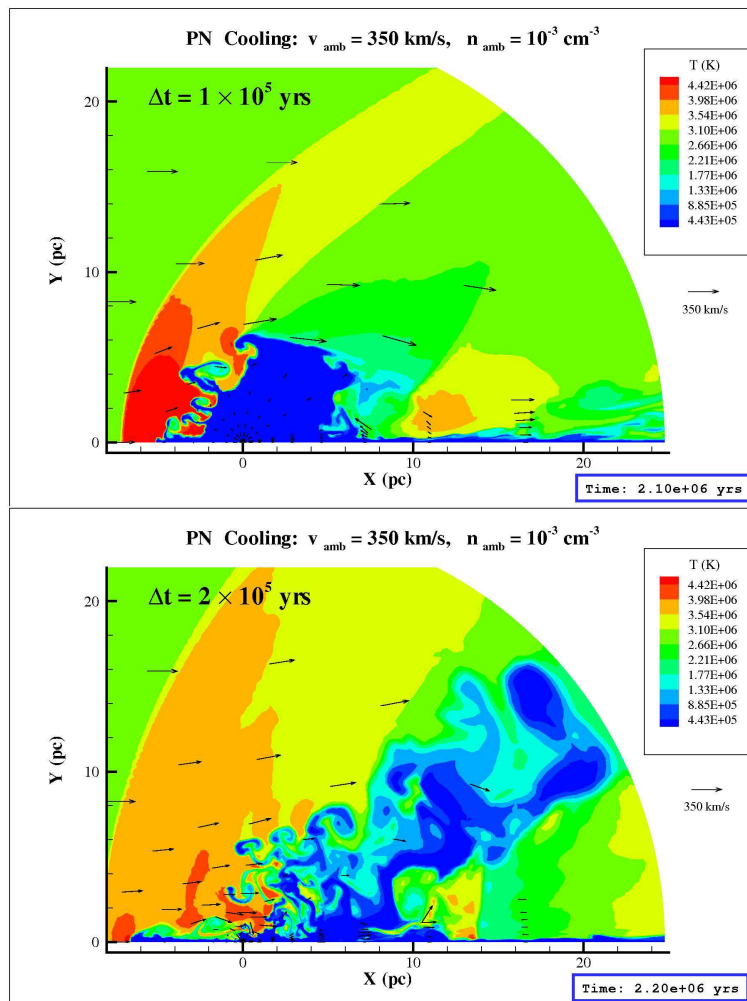


Fig. 10.— Large instabilities have begun nebula disruption by 10^5 years (top); the cooled case is much more unstable than the adiabatic case. The total disruption of the nebula is achieved by 2×10^5 years. The higher instability of the cooled case has made more material available for rapid transfer off the grid. These blobs are more separated from the axial wake flow. The mass of the majority of the disconnected material is $0.2M_{\odot}$, of which $0.02M_{\odot}$ has a temperature below 10^5 K, so it is colder than the blob in the non-cooling case. There is likely to be even more cooled PN material still in the slower-moving wake. Also, the upstream symmetry axis instability has been amplified by the larger mass outflow.

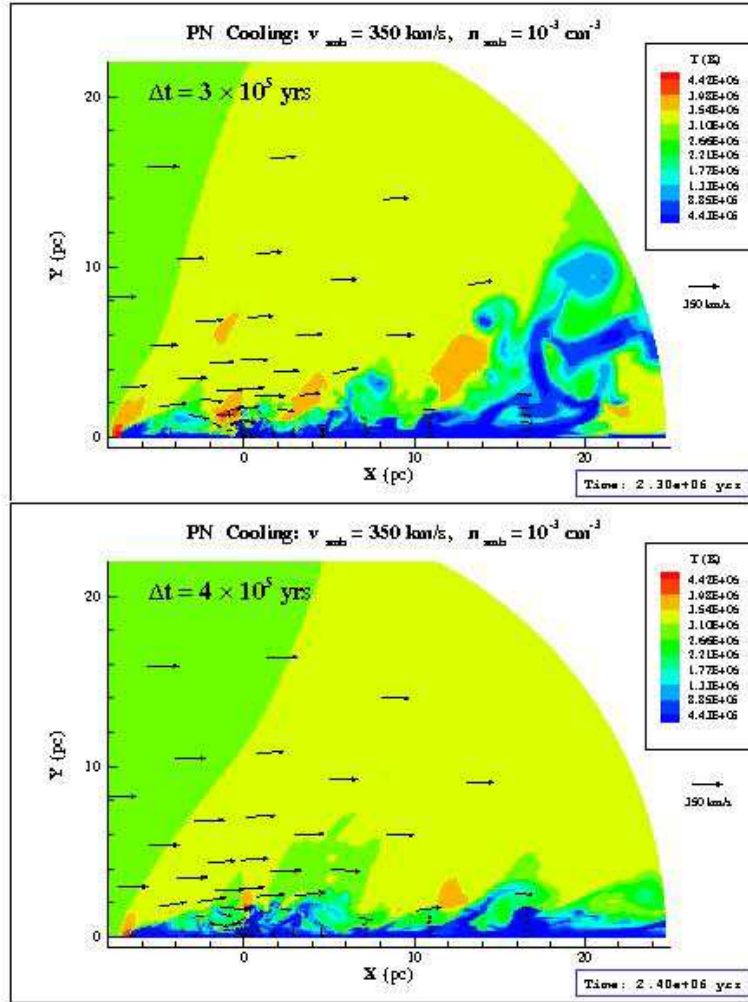


Fig. 11.— The last of the larger cooled structures will exit the grid soon after 3×10^5 years (top), and the only remaining cooled PN material at 4×10^5 years (bottom) is in the narrow wake region.

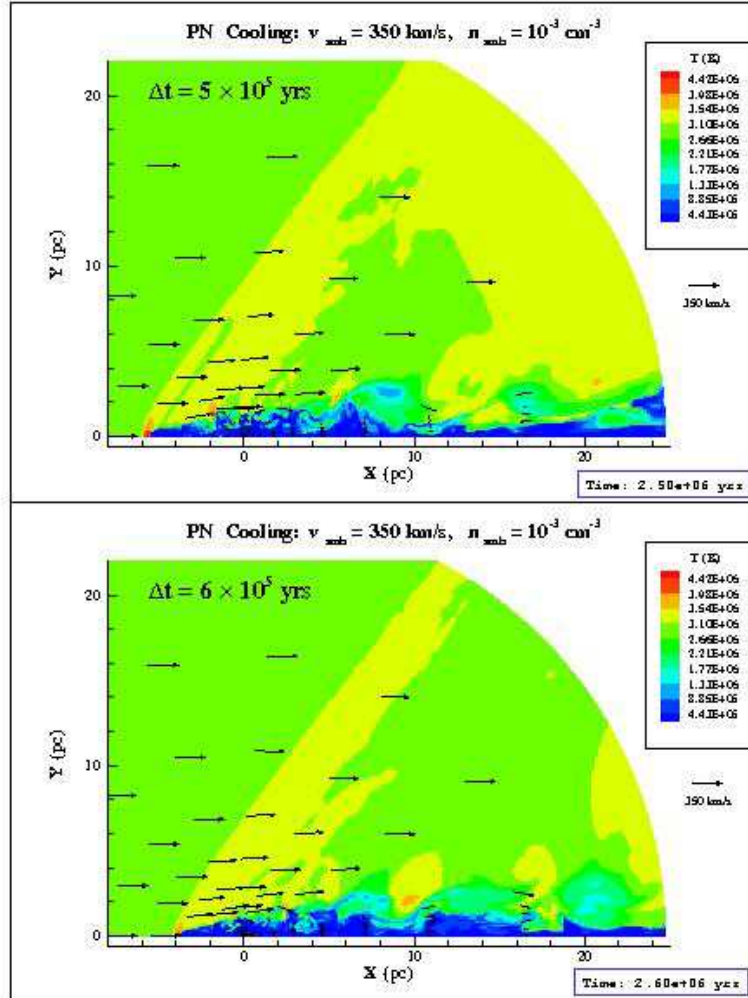


Fig. 12.— The flow has returned to the pre-PN state, although more material may remain in the cooled slow wake.

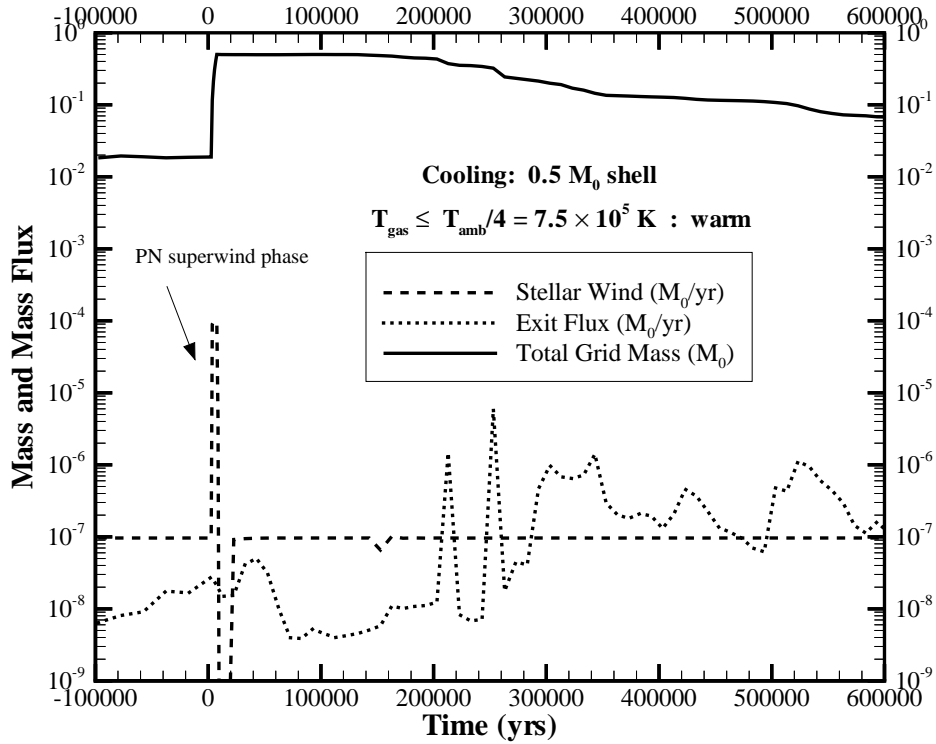


Fig. 13.— Mass fluxes for warm $< T_{\text{amb}}/4$ K gas in the simulations with radiative with cooling. This gas is quickly accelerated and advected off the grid by the ambient flow, so that the warm gas is gone by 3.5×10^5 years. The dip after the superwind is a numerical artifact.

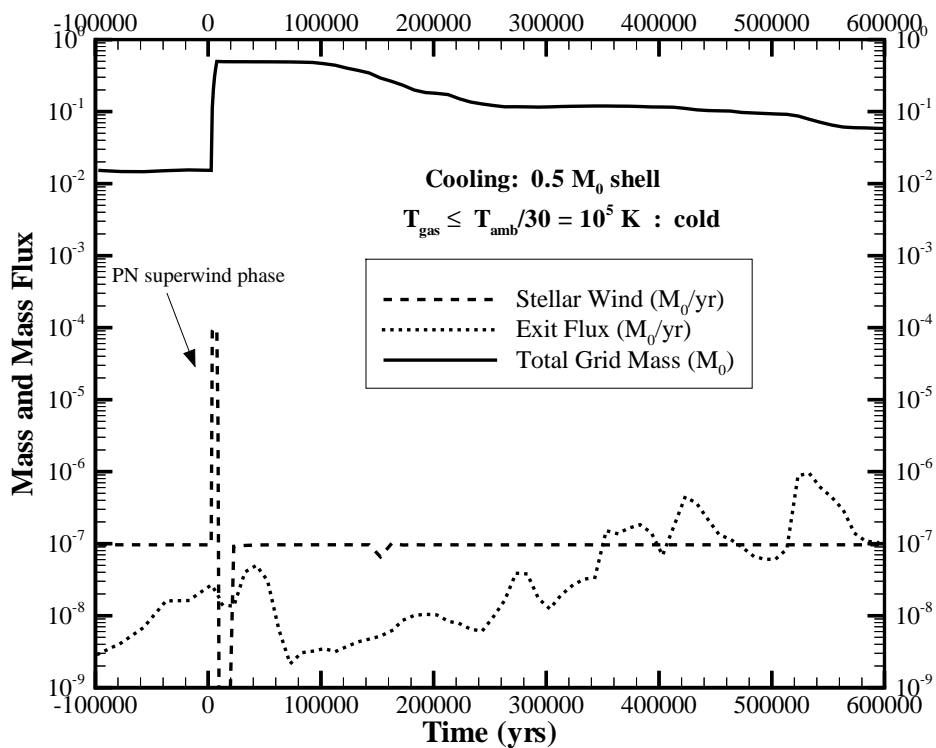


Fig. 14.— Mass fluxes for colder $< T_{\text{amb}}/30 \text{ K}$ gas with cooling. The total mass and exiting mass flux curves suggest that the radiative cooling has managed to cool the wake, and in this case any PN material in the slower wake region appears to have been trapped there through cooling induced accretion.

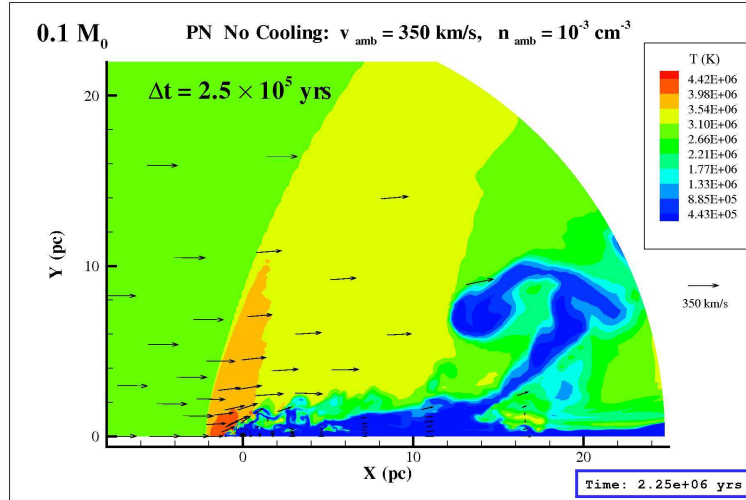


Fig. 15.— The bulk of the smaller PN shell just prior to exiting the grid, at 2.5×10^5 years after the initial superwind phase. The smaller mass nebula evolution is remarkably similar to the larger mass case: compare this temperature map to the top panel in Figure 4. The general character of the mushroom shape is the same, although the size of the structure is correspondingly reduced.

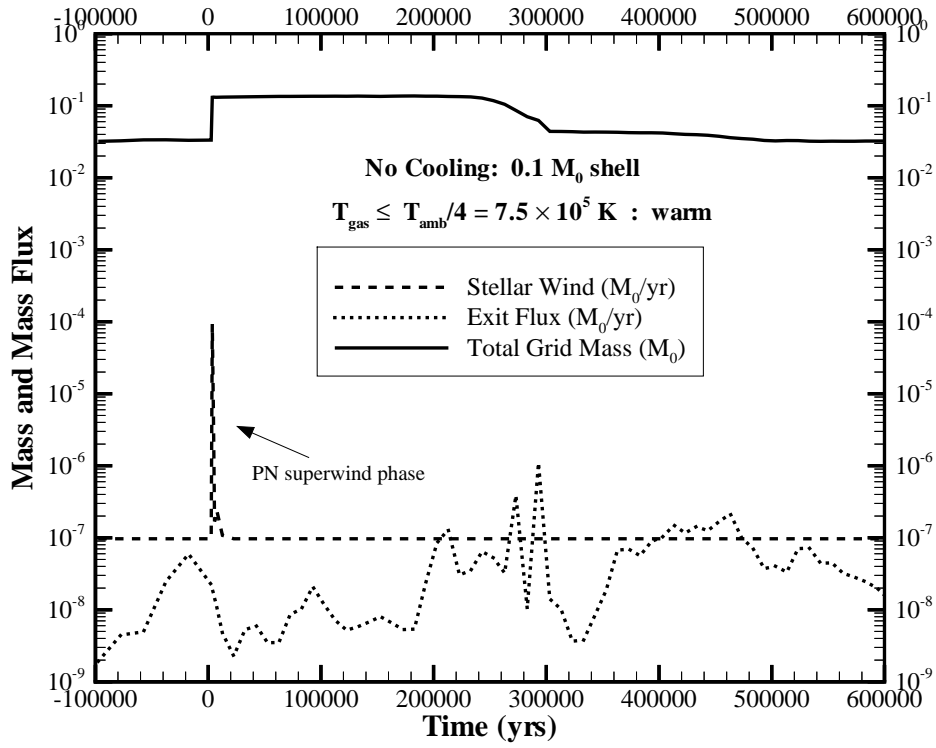


Fig. 16.— $0.1M_{\odot}$ mass fluxes for warm $< T_{\text{amb}}/4$ K gas, showing a quicker advection of the PN material off the grid, and two main parcels of gas which leave the grid just after 2.5×10^5 years. These two larger parcels are shown in Figure 15.

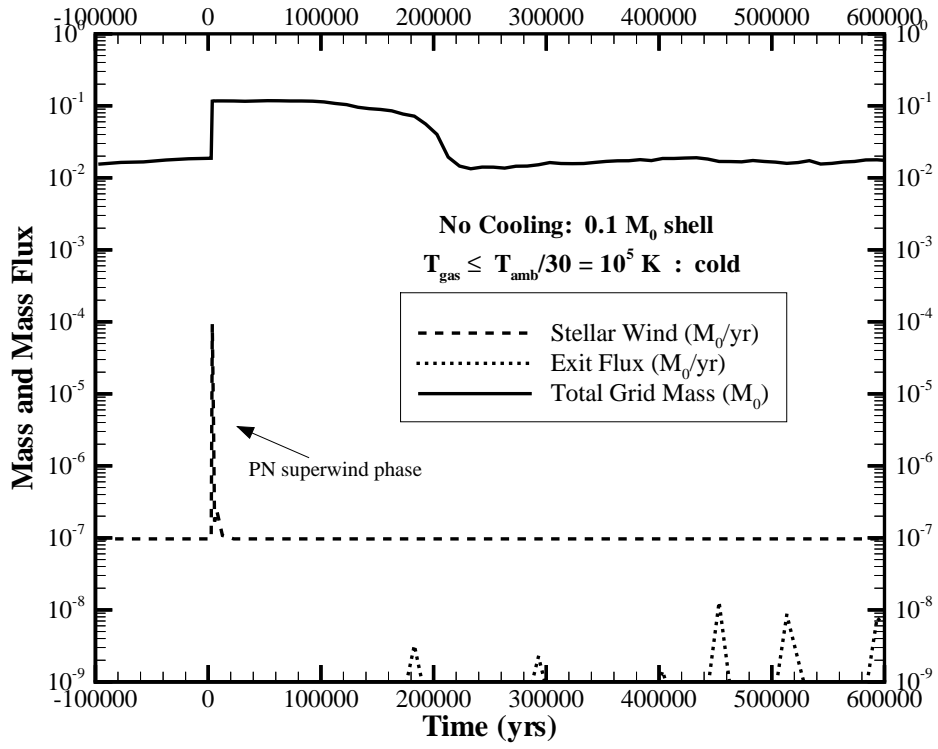


Fig. 17.— $0.1M_{\odot}$ mass fluxes for colder $< T_{\text{amb}}/30$ K gas, showing the same heating effects as the larger mass nebula.

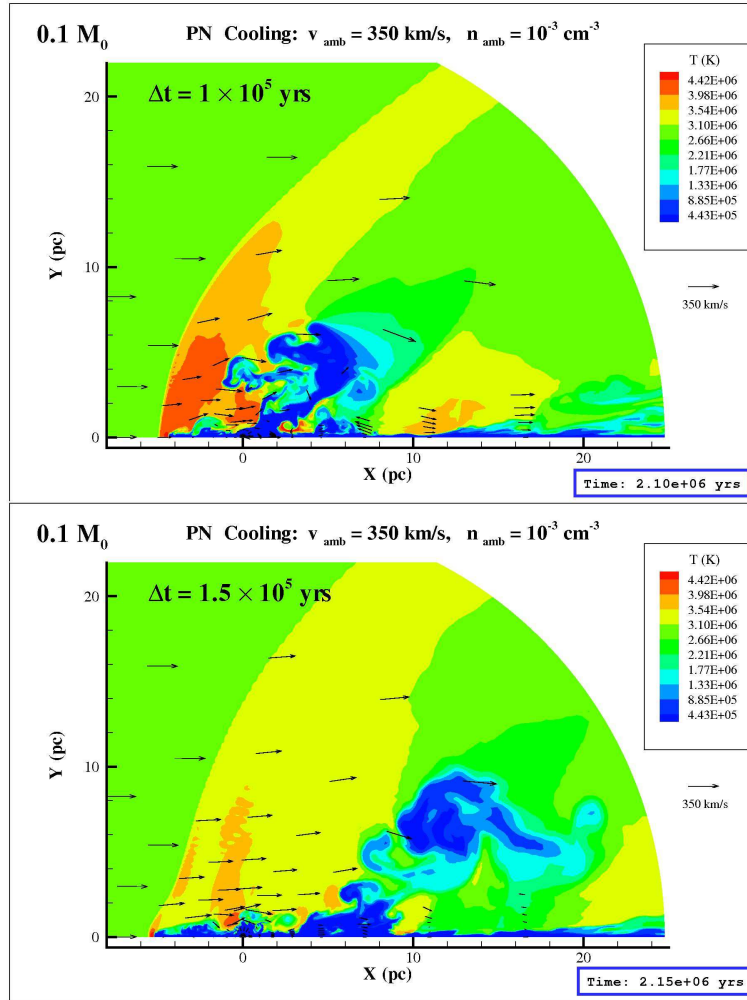


Fig. 18.— Typical cooled instabilities and disruption of the PN. At 10^5 years, the PN is in process of breaking apart, and by 1.5×10^5 years a large blob has broken off completely. This blob is quickly moving off the grid, and will be gone just after 2×10^5 years.

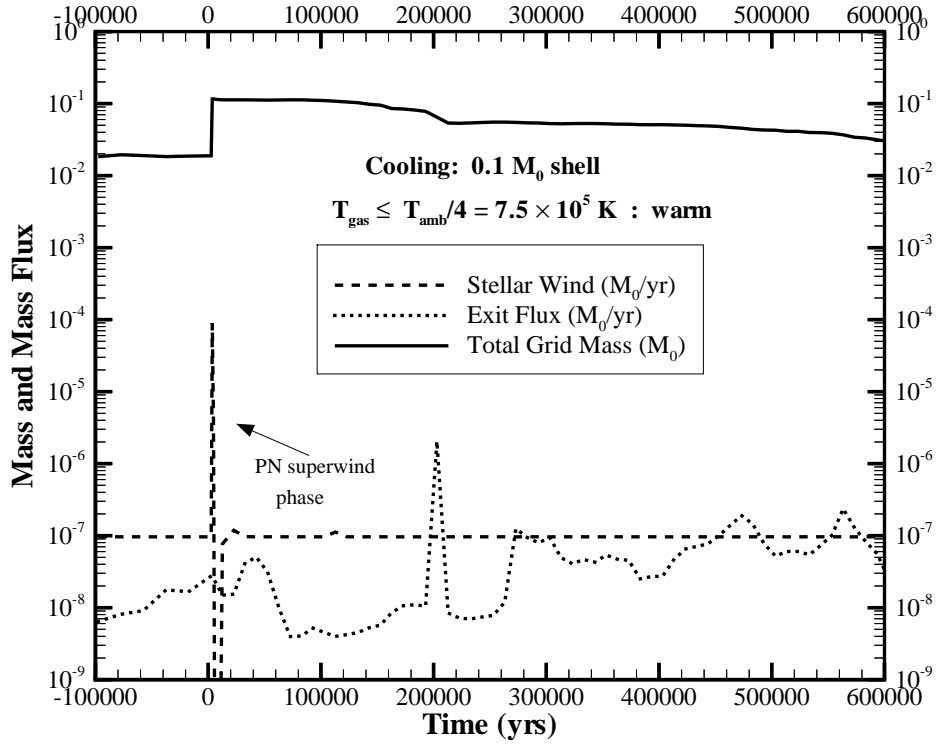


Fig. 19.— $0.1M_{\odot}$ mass fluxes for warm $< T_{\text{amb}}/4$ K gas in the simulations with radiative cooling. The majority of warmer gas that leaves the grid does so in the large broken-off parcel of gas that shows up as a sharp peak in the exiting mass flux curve just after 2×10^5 years. The cooling has also hastened the departure of the warm gas compared to the adiabatic case.

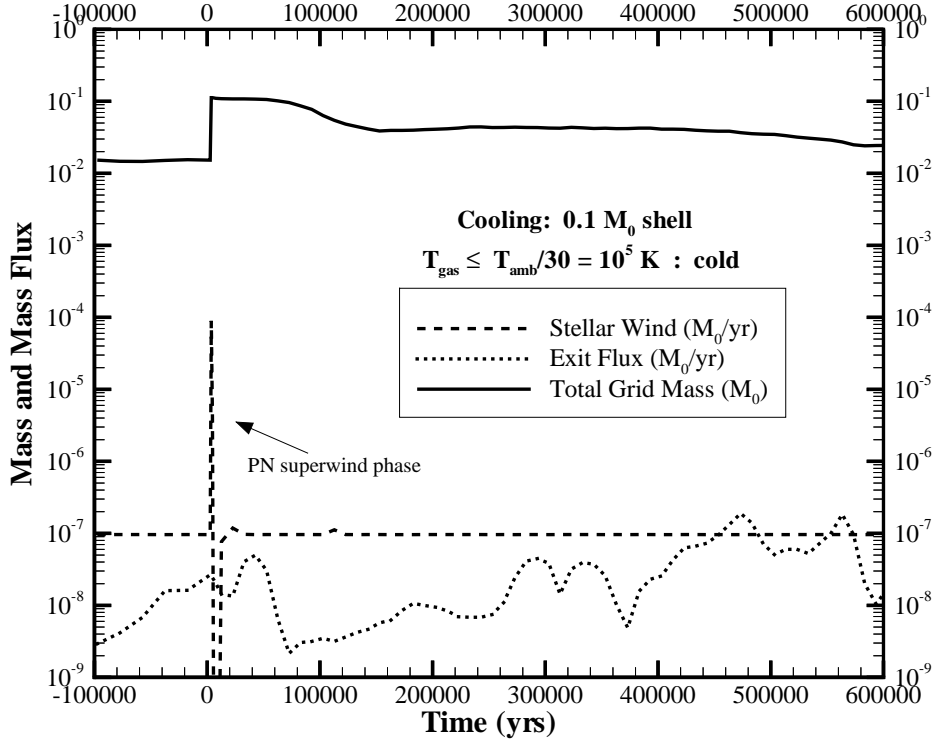


Fig. 20.— $0.1M_{\odot}$ mass fluxes for colder $< T_{\text{amb}}/30$ K gas in the simulations with radiative cooling. With the exception of the large warm parcel that quickly leaves the grid, remaining PN material flows along the narrow wake and continue to cool until it leaves the grid. The exiting mass flux curve is almost the same as in the warmer case, which indicates that nearly all wake material leaving the grid is cold. The coldest ejecta is heated in the first 10^5 years, which is comparable to the radiative cooling time.